

Next Generation Very Large Array Memo #85

Comparison of Alternative Configurations for the ngVLA Plains Subarray

Viviana Rosero (NRAO), Joe Carilli (NRAO), Chris Carilli (NRAO),
& Brian Mason (NRAO)

October 20, 2020

Abstract

We consider the performance of two alternative configurations to the ngVLA Plains (5-arm spiral) subarray, with both subarrays redistributing a third of the collecting area from the Core to the Plains. One involves a 7-arm spiral, and the second a 5-arm spiral in which one station along each arm is a cluster of six or seven antennas, which we designate the ‘Lily Pad’ subarray. In terms of the naturally weighted PSF skirt, we find a factor 2 decrease in the level of the naturally weighted skirt when including the remaining Core antennas, for both the 7-arm and Lily pad configurations (64 antennas in the core), relative to the original 5-arm spiral. This improvement is due to the lower number of antennas in the core relative to the longer baselines (94 antennas in the core). Likewise, both arrays with more antennas at longer baselines show improved synthesized beam performance in terms of taperability. Considering uniform weighted imaging of a complex, extended source that requires very high dynamic range, and including the Core, all the configurations produce high dynamic range images, with the 7-arm spiral providing the best results, by a factor 1.5 to 2. In section 3, all comparisons were made with the same number of antennas (i.e., 5-arm spiral is the current Plains+Core subarray, 7-arm spiral and Lily Pad configurations both have the remainder of the Core). The dynamic ranges vary from 6000 for snapshot observations using the original 5-arm spiral and Lily pad configurations, to close to 10^5 dynamic range for a 6hr synthesis observation using the 7-arm spiral. In terms of image fidelity, we find that for a 6 hour track all considered configurations would deliver accurate imaging at the 0.5% level (0.995 or better by the fidelity metric adopted by the ngVLA project). The RMS of per-pixel fidelity is comparable for the current 5-arm spiral and the 7-arm spiral, with the Lily pad worse by a factor of 1.5. Results are similar for 10 minute snapshot images: all configurations yield fidelities 0.994 or better, but in this case the fidelity RMS of the 7-arm configuration is 2.2 and 3 times lower, respectively, than the current 5-arm and Lily pad arrays. All arrays considered accurately reconstructed total fluxes of structures up to $40''$ in size to better than 1% in most cases. For snapshot observations the current 5-arm and Lily pad arrays perform slightly better than the 7-arm array, presumably due to the smaller number of short baselines present in the latter; however, all arrays performed comparably for a 6 hour track.

1 Introduction

We explore two alternatives to the current Rev-C 5-arm spiral on the Plains of San Augustin, with a focus on improved image quality for imaging with baselines out to 37 km. We consider two metrics: (i) synthesized beam shape and taperability, and (ii) image dynamic range and fidelity when imaging an extended, complex source requiring high dynamic range.

Taperability curves, or the change in sensitivity versus resolution, can be used to compare arrays and to understand how efficiently an array can perform at both high and low resolutions (ngVLA memos #55 [5] and #72 [6]). The ngVLA reference design has a large ratio of short to long baselines which is what allows it to accommodate a wide range of resolutions without losing too much sensitivity, but with a resulting naturally-weighted PSF that has an undesirable, broad skirt. In consequence, sculpting of the synthesized beam may be necessary in order to meet specific science requirements, e.g., image fidelity.

As documented in ngVLA memo #76 [7] the associated sensitivity penalty of sculpting of the synthesized beam is more severe for a broader skirt. Therefore, we are in the process of identifying and studying alternative subarrays that ‘naturally’ produce a more Gaussian PSF and that are yet efficient over a wide range of resolutions. In this memo we present the taperability curve, 1D East-West cuts through the naturally weighted PSF and distribution of baseline lengths for new subarrays (i.e., 7-arm spiral subarray and Lily Pad subarray). Additionally, we measure and analyze the image fidelity for simulated images using the alternative configurations and compared them with the 5-arm spiral.

As a test of pure imaging performance, we include an analysis of a complex, extended source with regions of very high surface brightness. In this case, uniform weighting is warranted, since the image noise is dominated (by orders of magnitude), by image artifacts due to the very high surface brightnesses, even for dynamic ranges approaching 10^5 .

2 Taperability and Performance Analysis

In this part of the analysis for the simulations, we generated visibilities with the CASA `sm` toolkit using both a 4 hr (long track) and a 60 second (snapshot) observation time. The simulations are centered on the transit of a single field at +24 declination, with a central frequency of 30 GHz and are composed of a single channel and an integration time of 1 second. No source visibilities were predicted, i.e., each simulation is of a blank field. An arbitrary amount of thermal noise was added to the visibilities using the `sm.setnoise` function of the CASA simulation toolkit. Please refer to ngVLA memos #55 [5], #72 [6] and #76 [7] for a detailed description of the type of simulations made in order to create the taperability curves presented in this document. The imaging was done using the CASA task `tclean` and all the simulated images have an image size of 4096 pixels. The chosen cell size is 0.4 times the value supplied by `im.advise`, such that the resolution of the longest baseline is oversampled by a factor of 5. For this specific case the cell size is 0.011 arcsec, given that both subarrays have the same value for their longest baseline.

2.1 7-arm Spiral Subarray

The Plains alone subarray is composed of 74 18 m antennas (see Figure 1 left) and has a 5-arm spiral morphology, log SKA-type spiral, as described in memo #82 [2]. The Plains subarray extends over a maximum baseline of 36.7 km and a minimum baseline of 275 m. The 7-arm Spiral alternative subarray is composed by the Plains alone (i.e., the same log spiral but with 7 arms of 15 antennas each) plus $\sim 30\%$ of the Core antennas selected randomly and moved to the Plains (see Figure 1 right) for a total of 105 18 m antennas.

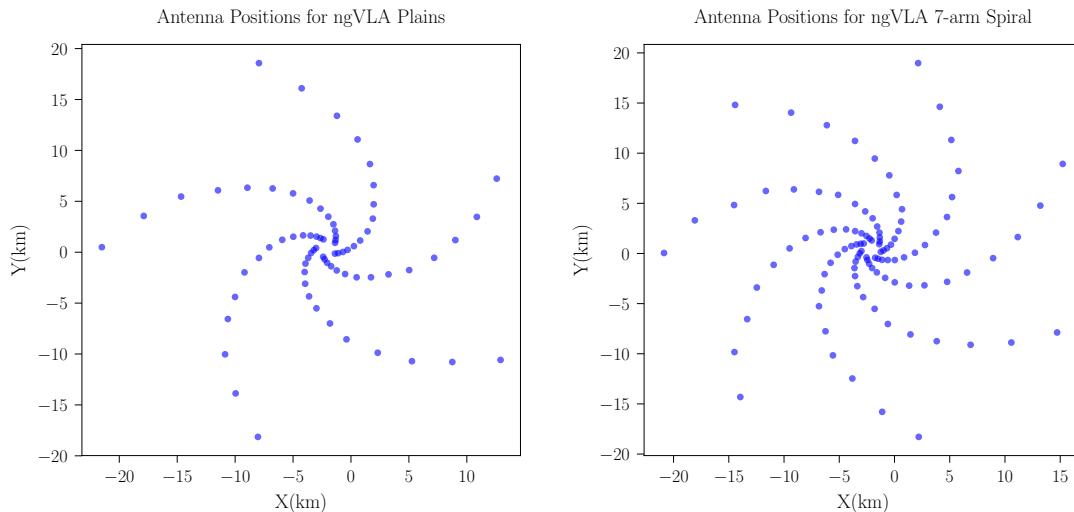


Figure 1: Positions of the 74 18 m antennas for the Plains subarray (left) and the 105 18 m antennas of the 7-arm spiral (right).

Three cases are analyzed:

- Case 1: Plains+Third Core versus 7-arm Spiral
- Case 2: Plains versus 7-arm Spiral
- Case 3: Plains+Core versus 7-arm Spiral+rest of the Core

2.1.1 Case 1: Plains+Third Core versus 7-arm Spiral

Since the Plains-7 arm has $\sim 30\%$ of the Core we decided to compare it with the Plains+Third Core subarray¹, *so they have about the same number of antennas*.

The taperability results show that the Plains+Third Core subarray is taperable to lower resolutions but has a higher skirt at higher resolutions, all as a consequence of having a larger ratio of shorter to larger baselines (see Figure 2). At the highest resolutions using

¹This is the same subarray studied in ngVLA memo 72

robust weighting the 7-arm Spiral obtains slightly higher resolution. The snapshot results for all the configurations shown in this document show that robust weighting does not achieve as high resolutions or (as high inefficiencies) as in the case of the longer tracks (see Figure 3). The 1D East-West cuts through the naturally weighted PSFs are seen in Figure 3 (right) and they seem acceptable.

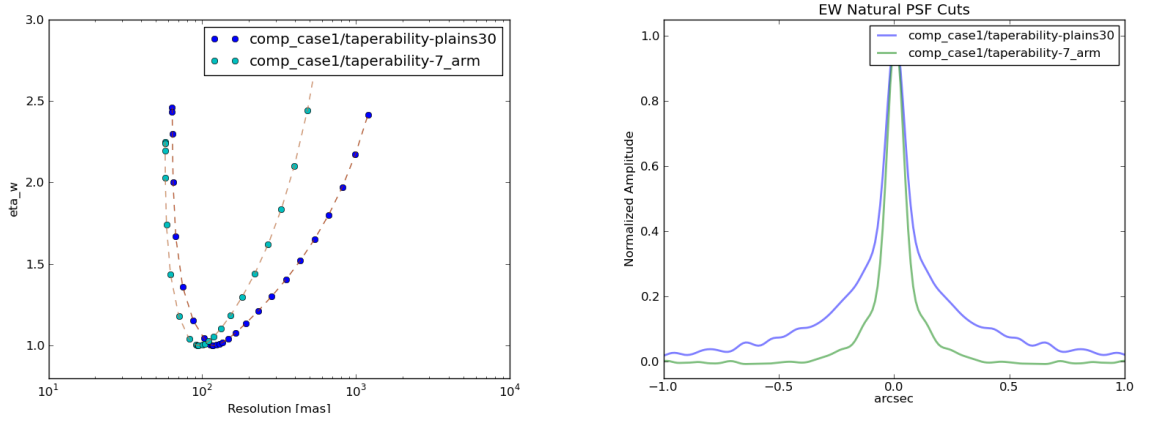


Figure 2: Taperability curves (left) and 1D East-West cuts through the naturally weighted PSFs for both subarrays in case 1 for a long track.

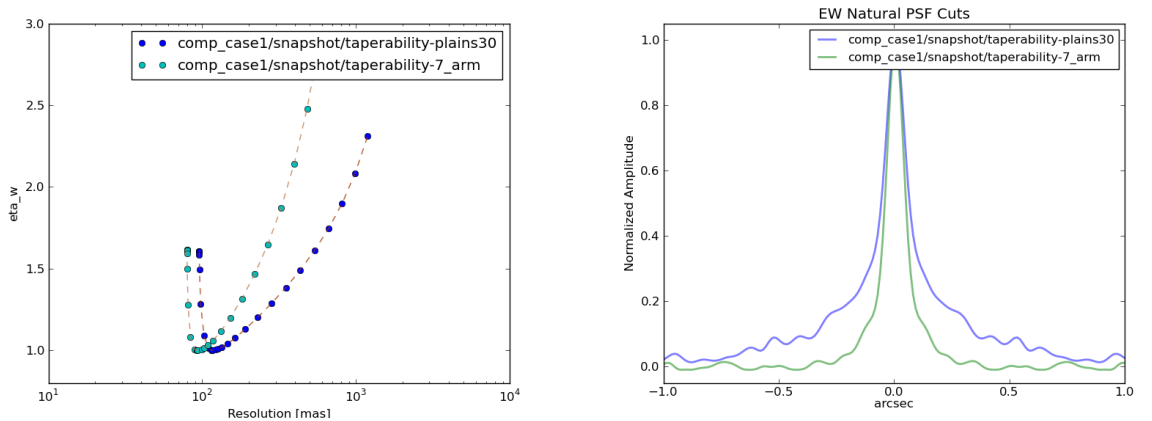


Figure 3: Taperability curves (left) and 1D East-West cuts through the naturally weighted PSFs for both subarrays in case 1 for a snapshot.

Figure 4 shows distribution of baseline lengths for the two subarrays. The 7-arm Spiral does not have that many short baselines which is expected since it does not have antennas from

the Core. Additionally, the 7-arm Spiral provides more longer baselines because it has more antennas in the Plains.

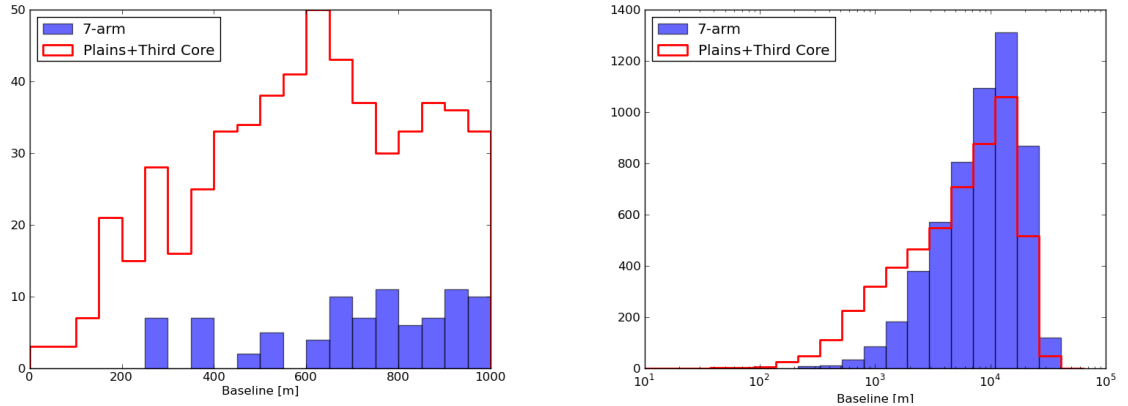


Figure 4: Distribution of baseline lengths for Plains+Third Core versus 7-arm Spiral for baseline lengths of 1000 m (left) and 37.6 km (right) which is the maximum baseline length.

2.1.2 Case 2: Plains versus 7-arm Spiral

Same comparison than case 1 but without adding the $\sim 30\%$ of the Core antennas to the Plains. The taperability curves and the naturally weighted synthesized beams are very similar for both cases because they both have approximately the same shortest and longest baselines and they have about the same distribution (see Figure 5 and 6). The only difference is the sensitivity since the 7-arm Spiral has more antennas (thus, 7-arm 42% more sensitive). Note that both taperability curves are normalized to the sensitivity at natural weighting.

Figure 7 shows distribution of baseline lengths for the two subarrays. The 7-arm Spiral has more short baselines, and overall it has more long baselines, but this is due to having more antennas.

2.1.3 Case 3: Plains+Core versus 7-arm Spiral+rest of the Core

In this case, the Plains subarray has all the Core antennas and the 7-arm Spiral has $\sim 60\%$ of the Core antennas, thus both subarrays have about the same total number of antennas (Plains+Core :168 18 m antennas; 7-arm Spiral+rest of the Core: 167 18 m antennas). The taperability curve for the 7-arm Spiral+rest of the Core is more efficient at higher resolutions. On the other hand, the Plains+Core is more efficient at lower resolutions but the naturally weighted synthesized beam has a higher skirt (see Figure 8 and 9).

Figure 10 shows distribution of baseline lengths for the two subarrays. The Plains+Core subarray appears to have a better distribution of short and long baselines than the 7-arm

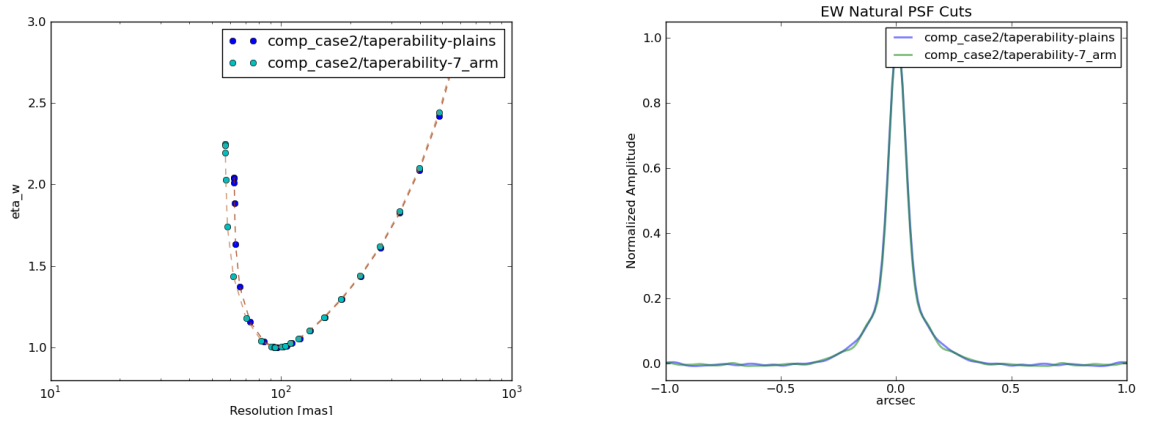


Figure 5: Taperability curves (left) and 1D East-West cuts through the naturally weighted PSFs for both subarrays in case 2 for a long track.

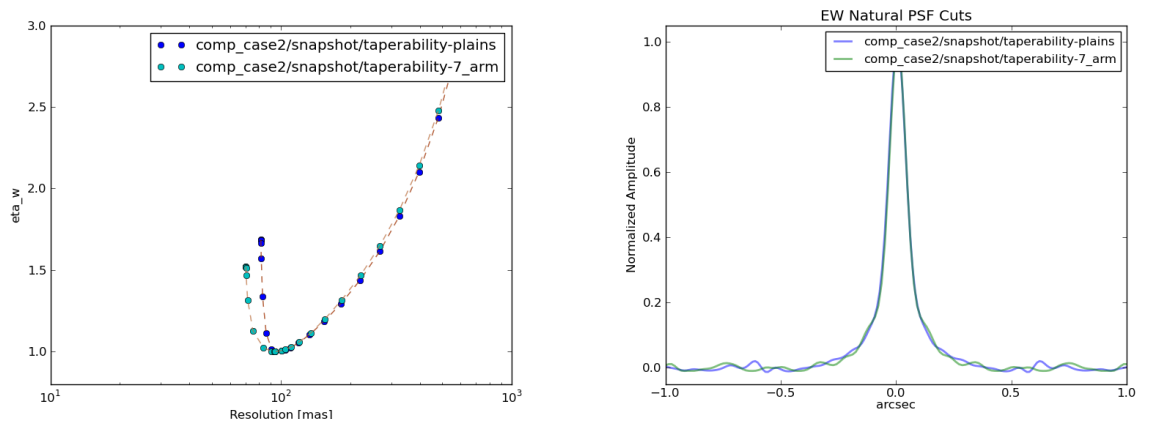


Figure 6: Taperability curves (left) and 1D East-West cuts through the naturally weighted PSFs for both subarrays in case 2 for a snapshot.

Spiral+rest of the Core.

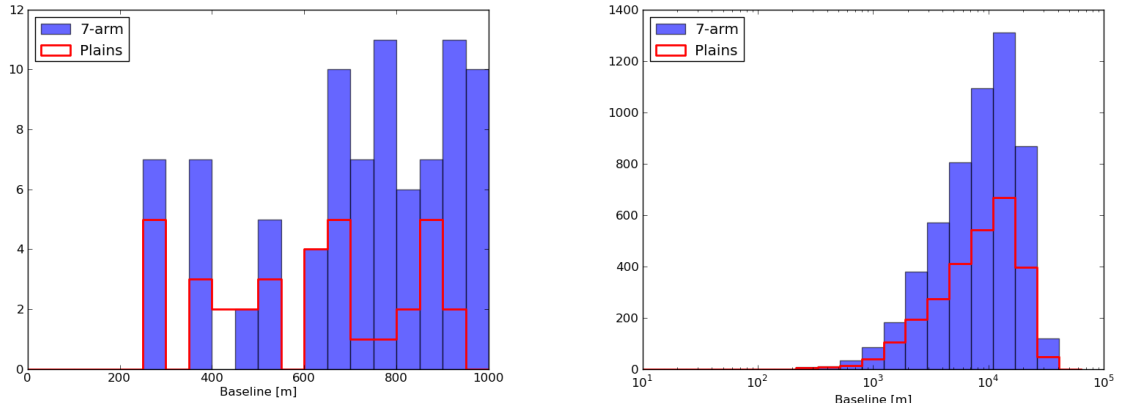


Figure 7: Distribution of baseline lengths for Plains versus 7-arm Spiral for baseline lengths of 1000 m (left) and 37.6 km (right) which is the maximum baseline length.

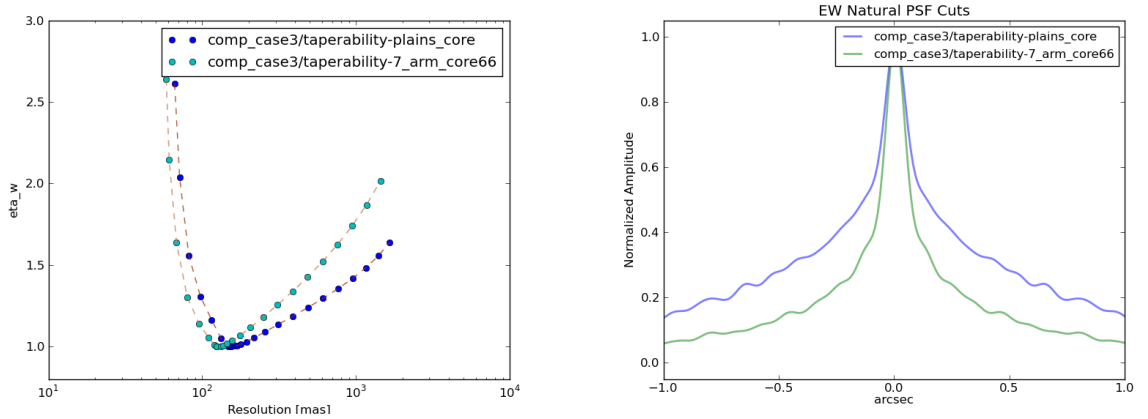


Figure 8: Taperability curves (left) and 1D East-West cuts through the naturally weighted PSFs for both subarrays in case 3 for a long track.

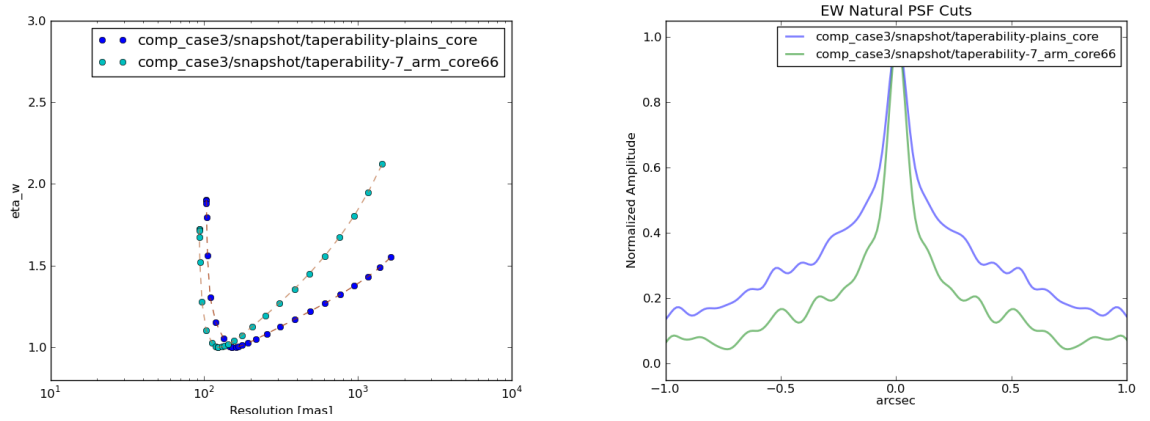


Figure 9: Taperability curves (left) and 1D East-West cuts through the naturally weighted PSFs for both subarrays in case 3 for a snapshot.

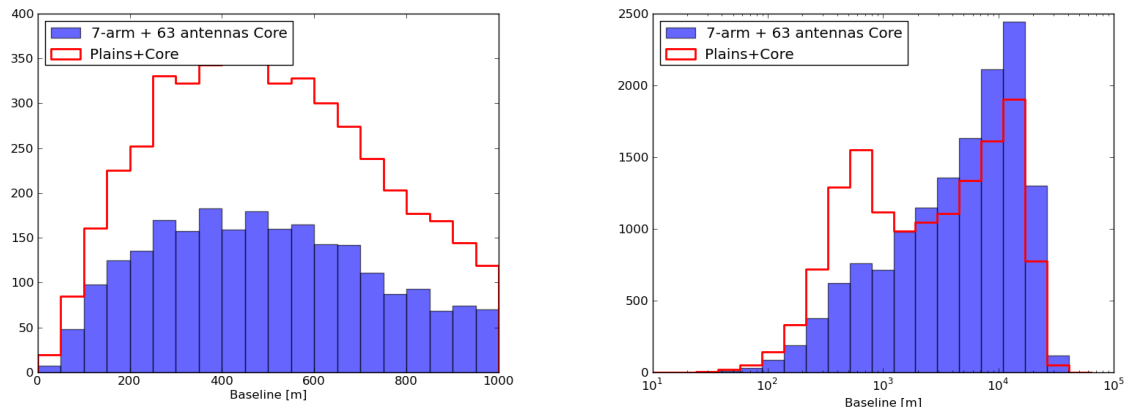


Figure 10: Distribution of baseline lengths for Plains+Core versus 7-arm Spiral+rest of the Core for baseline lengths of 1000 m (left) and 37.6 km (right) which is the maximum baseline length.

2.2 Lily Pad Subarray

The Lily Pad subarray is composed by the Plains alone plus $\sim 30\%$ of the Core antennas selected randomly and moved to the Plains in small semi-random clusters for a total of 101 18 m antennas. The pattern is one Lily Pad connected to the last antenna of one of the 5-arm spiral, and then the next Lily Pad on the next arm but moved one antenna in towards the center and so forth (see Figure 11 right). In this distribution we tried to have short baselines of the size of the minimum allowed distance (i.e., 38 m) and some baselines up to the length of the shortest baseline of the Plains alone (i.e., 275.12 m).

Four cases are analyzed:

- Case 1: Plains+Third Core versus Lily Pad subarray
- Case 2: 7-arm Spiral versus Lily Pad subarray
- Case 3: Plains+Core versus Lily Pad subarray+rest of the Core
- Case 4: 7-arm Spiral+rest of the Core versus Lily Pad subarray+rest of the Core

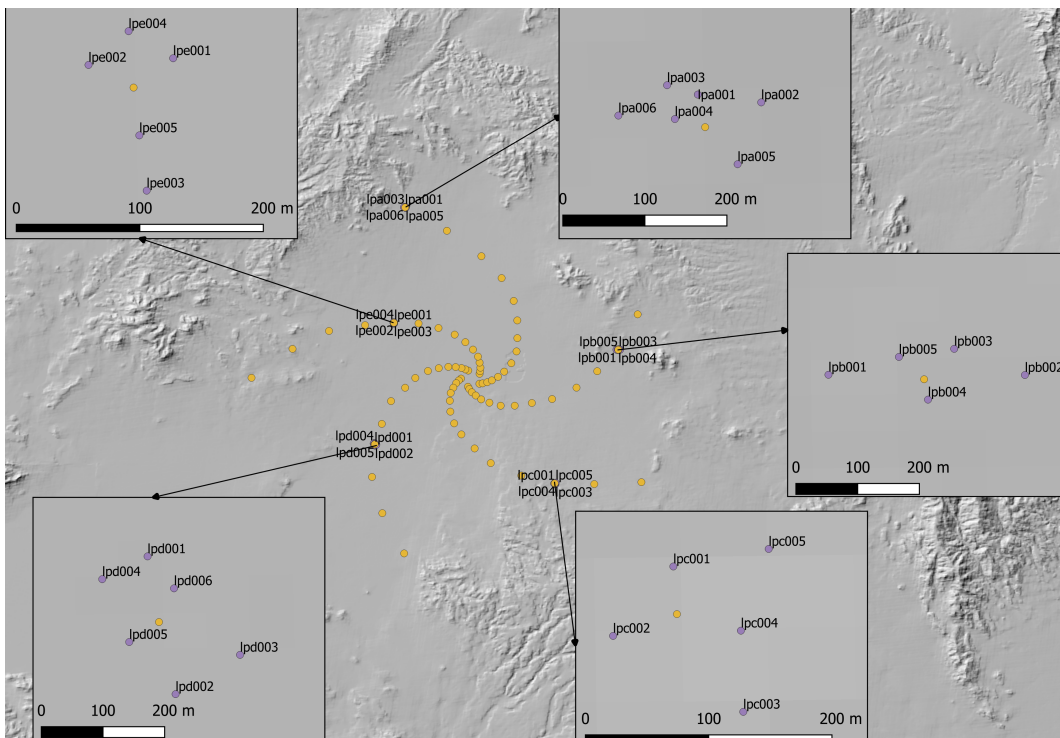


Figure 11: Positions of the 101 18 m antennas for the Lily Pad subarray.

2.2.1 Case 1: Plains+Third Core versus Lily Pad Subarray

Since the Lily Pad subarray has $\sim 30\%$ of the Core we decided to compare it with the Plains+Third Core subarray (similar to case2.1.1 in the previous section), *so they have about the same number of antennas*.

The taperability results for the long track (Figure 12) and the snapshot (Figure 13) are very similar to the ones obtain in the comparison for the Plains+Third Core versus 7-arm Spiral (see case 2.1.1). The 1D East-West cuts through the naturally weighted PSFs are seen figures 12 and 13 (right). The PSF cut for the Lily Pad subarray appears to have some slightly higher sidelobes that perhaps can be mitigated by a distribution of antennas having additional North-South baselines (currently it appears that several baselines in the N-S direction may be redundant and thus there are larger gaps in the uv-coverage).

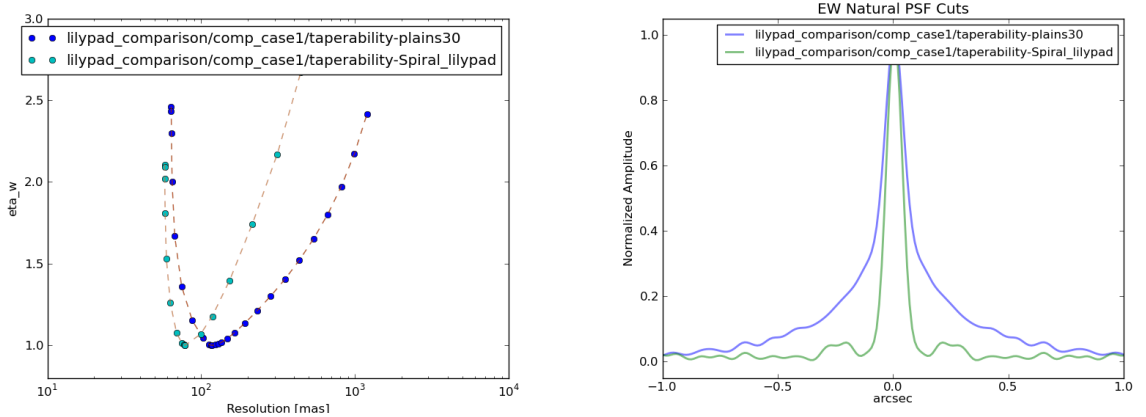


Figure 12: Taperability curves (left) and 1D East-West cuts through the naturally weighted PSFs for both subarrays in case 1 for a long track.

Figure 14 shows distribution of baseline lengths for the two subarrays. The Lily Pad subarray has at least 5 times more short baselines than the Plains+Third Core in the ~ 38 m to ~ 150 m range (this effect can be modified if the antennas in the Core are redistributed and carefully selected to include more shorter baselines). Additionally, the Lily Pad subarray provides more longer baselines, which is ideal for using this subarray as a stand alone subarray because Lily Pad it provides good LAS and long baselines coverage. Also, this will allow to use the left over antennas from the Core to work simultaneously on different observational projects.

2.2.2 Case 2: 7-arm Spiral versus Lily Pad Subarray

Similar comparison than case 1 where both subarrays *have about the same number of antennas*. The taperability curve is more efficient at lower (modest $\sim 100 - 500$ mas) resolutions for the 7-arm Spiral. The Lily Pad subarray has a higher native resolution (i.e., at natural weighting without taper), and is only very slightly more efficient at higher resolutions (see

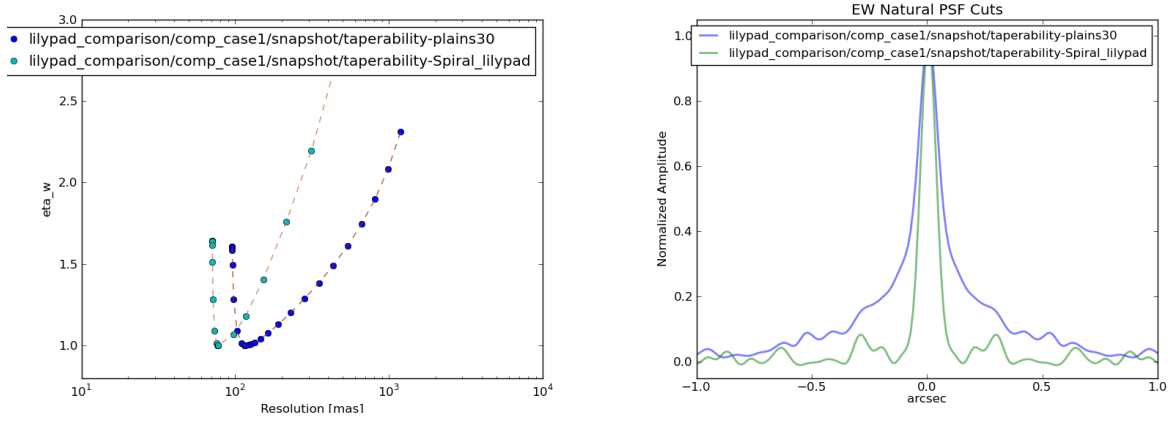


Figure 13: Taperability curves (left) and 1D East-West cuts through the naturally weighted PSFs for both subarrays in case 1 for a snapshot.

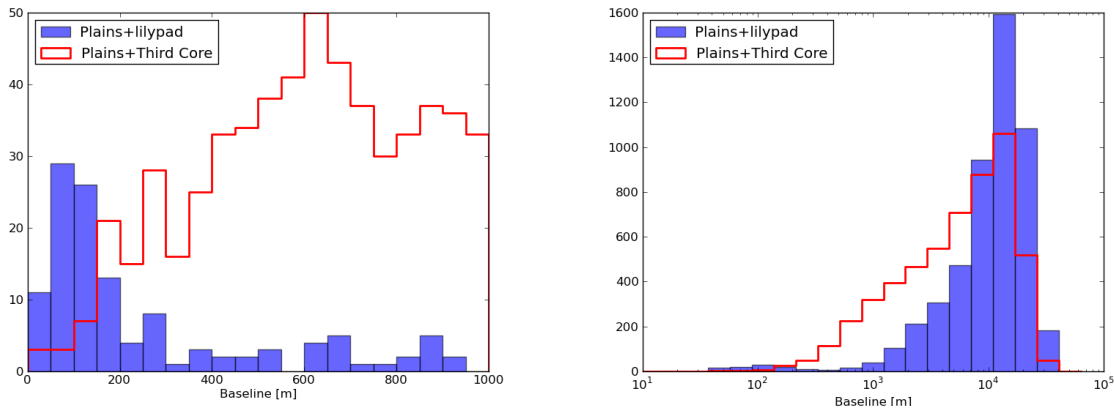


Figure 14: Distribution of baseline lengths for Plains+Third Core versus Lilypad subarray for baseline lengths of 1000 m (left) and 37.6 km (right) which is the maximum baseline length.

Figure 15 and 16 left panels). The 1D East-West cuts through the naturally weighted PSFs are seen figures 15 and 16 (right panels), where the synthesized beam for the Lily Pad subarray appears to be slightly better.

Figure 17 shows distribution of baseline lengths for the two subsets. The Lily Pad subarray offers a better LAS coverage than the 7-arm Spiral.

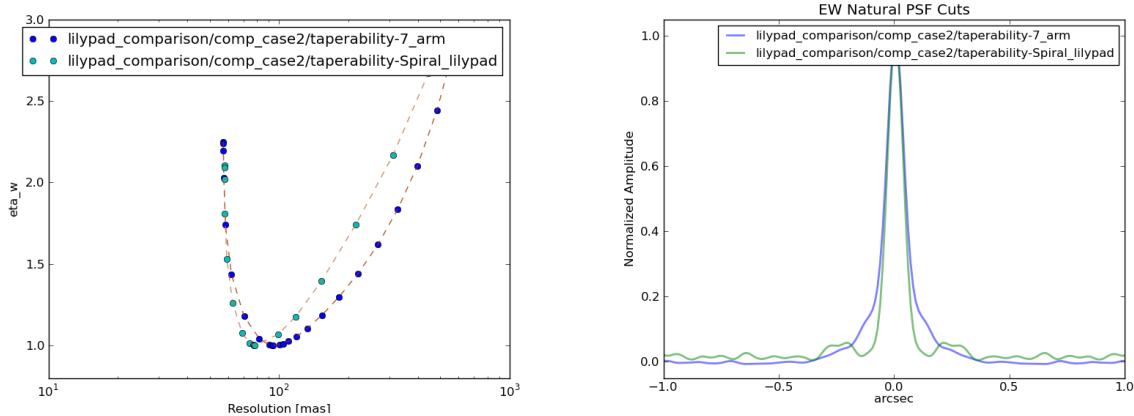


Figure 15: Taperability curves (left) and 1D East-West cuts through the naturally weighted PSFs for both subarrays in case 1 for a long track.

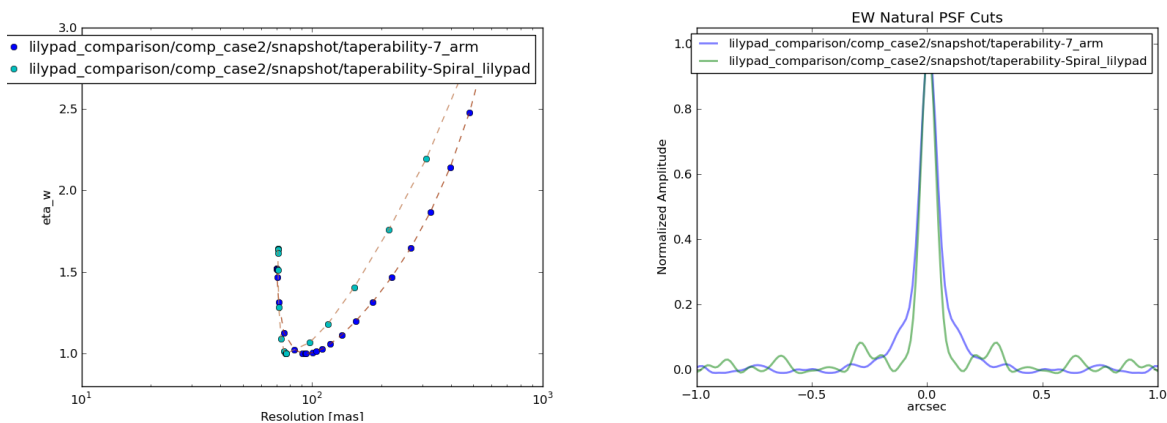


Figure 16: Taperability curves (left) and 1D East-West cuts through the naturally weighted PSFs for both subarrays in case 2 for a snapshot.

2.2.3 Case 3: Plains+Core versus Lily Pad Subarray+rest of the Core

In this case, the Plains subarray has all the Core antennas and the Lily Pad subarray has $\sim 60\%$ of the Core antennas, thus both subarrays have about the same total number of antennas (Plains+Core :168 18 m antennas; Lily Pad subarray+rest of the Core: 163 18 m antennas).

The taperability curve for the Lily Pad subarray+rest of the Core is more efficient at higher resolutions. However, the Plains+Core is more efficient at lower resolutions but the naturally weighted synthesized beam has a higher skirt (see Figure 21 and 19).

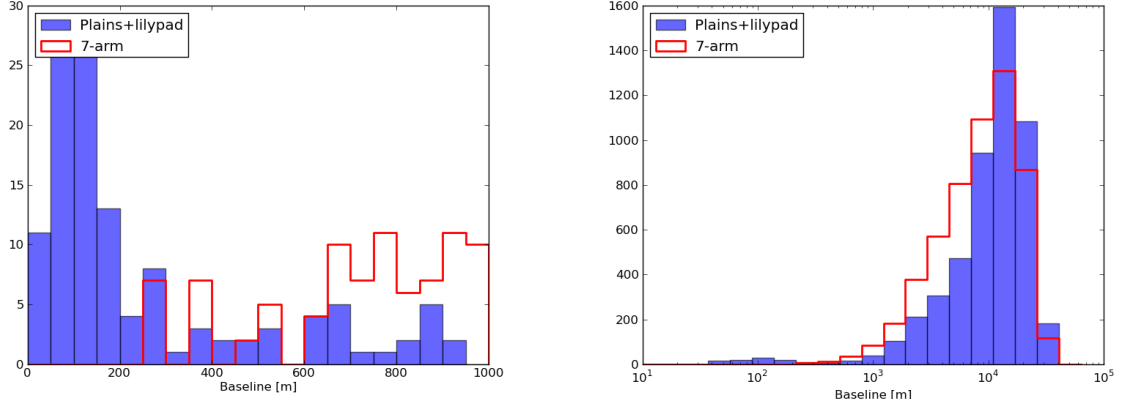


Figure 17: Distribution of baseline lengths for 7-arm Core versus Lilypad subset for baseline lengths of 1000 m (left) and 37.6 km (right) which is the maximum baseline length.

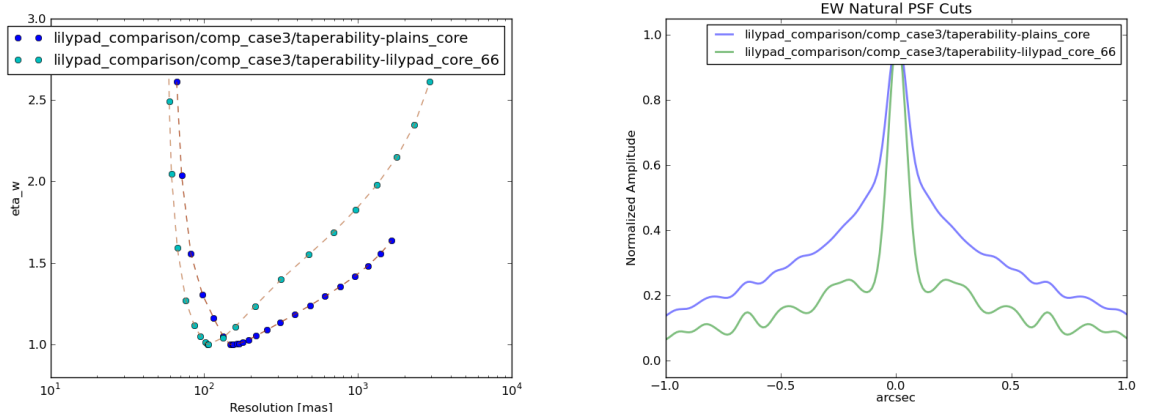


Figure 18: Taperability curves (left) and 1D East-West cuts through the naturally weighted PSFs for both subarrays in case 3 for a long track.

Figure 20 shows distribution of baseline lengths for the two subarrays. The Plains+Core subarray appears to have a better distribution of short and long baselines than the Lily Pad subarray+rest of the Core.

2.2.4 Case 4: 7-arm Spiral+rest of the Core versus Lily Pad Subarray+rest of the Core

The taperability curves and the naturally weighted synthesized beams are very similar for both cases because they both have approximately the same shortest and longest baselines and they have about the same distribution (see Figure 21 and 19).

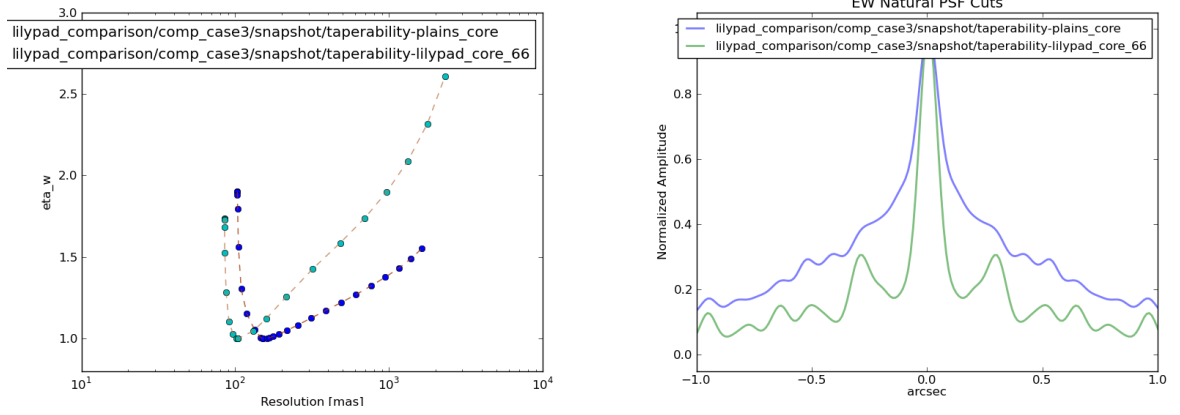


Figure 19: Taperability curves (left) and 1D East-West cuts through the naturally weighted PSFs for both subarrays in case 3 for a snapshot.

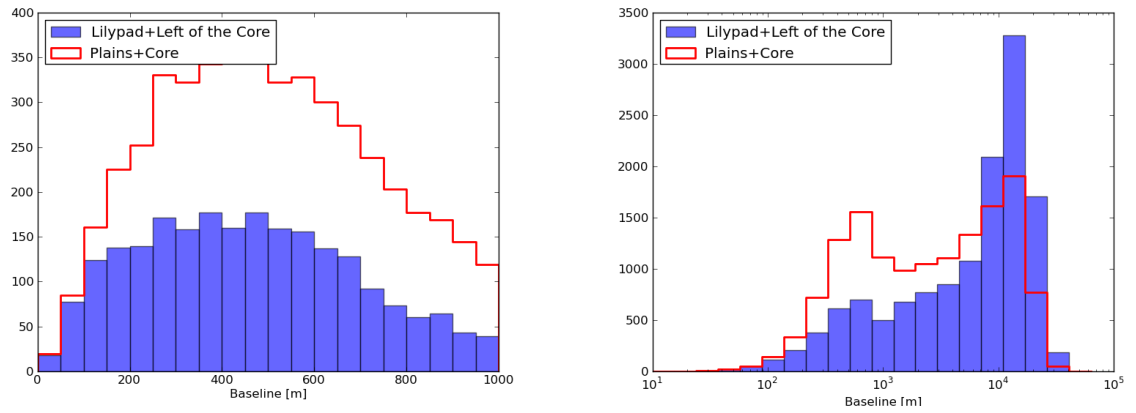


Figure 20: Distribution of baseline lengths for Plains+Core versus Lily Pad subarray+rest of the Core for baseline lengths of 1000 m (left) and 37.6 km (right) which is the maximum baseline length.

Figure 23 shows distribution of baseline lengths for the two subarrays.

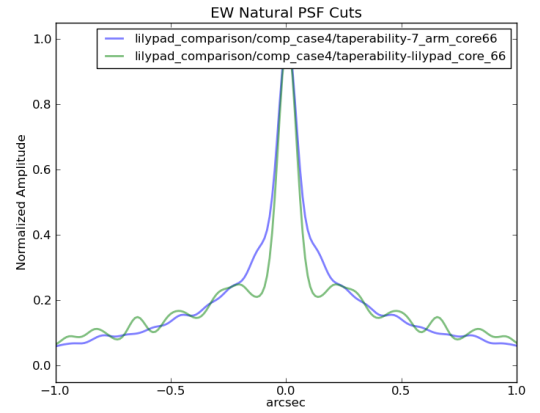
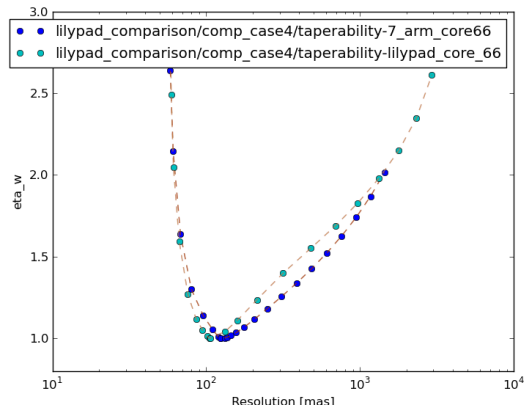


Figure 21: Taperability curves (left) and 1D East-West cuts through the naturally weighted PSFs for both subarrays in case 4 for a long track.

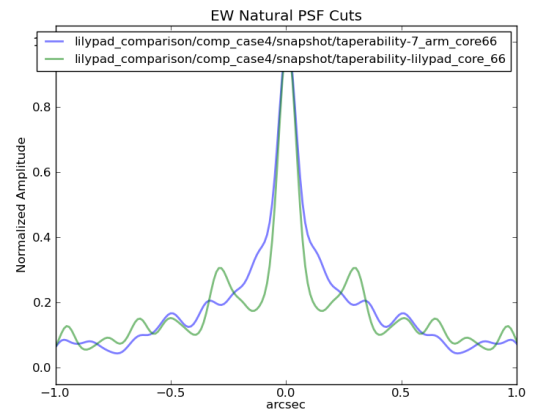
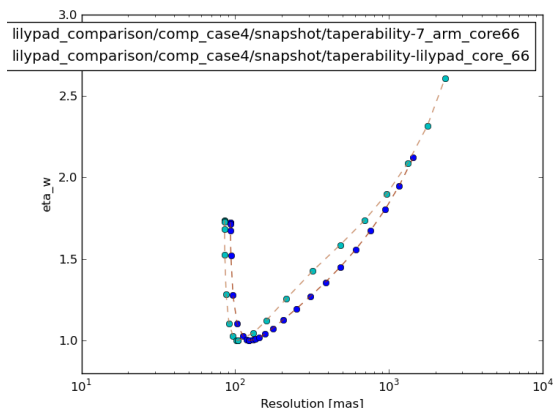


Figure 22: Taperability curves (left) and 1D East-West cuts through the naturally weighted PSFs for both subarrays in case 4 for a snapshot.

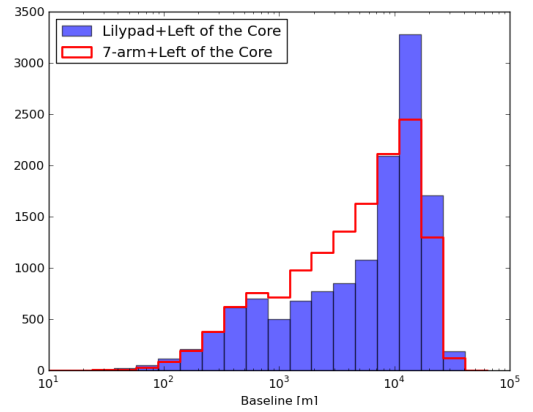
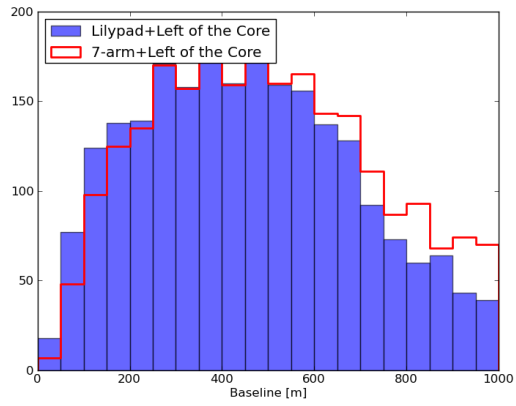


Figure 23: Distribution of baseline lengths for 7-arm Spiral+rest of the Core versus Lily Pad subarray+rest of the Core for baseline lengths of 1000 m (left) and 37.6 km (right) which is the maximum baseline length.

3 Image Fidelity

In this section we consider image fidelity when imaging a complex, extended object requiring high dynamic range. In this case, thermal noise becomes irrelevant, since the noise in the final image is dominated by imaging artifacts due to very high surface brightness regions in the complex source.

The model we employ is the same as was employed in the ngVLA memo #64 [1] to study the imaging fidelity of the 5-arm spiral (i.e., the configuration with the current Plains sub-array). The model involves an 8 GHz image of Cygnus A from the VLA, scaled in angle and processed in other ways described in memo #64 [1], to provide a good test of image fidelity of the ngVLA. The focus of this section is image dynamic range and fidelity, not noise limits and beam shape, hence we limit the analysis to Uniform weighting (with modest uv-tapering if needed to get similar resolutions, as described in memo #64 [1]). We do not include noise in the simulation. In all cases, we augment the configuration with the remaining 64 antennas in the Core. Given the uniform weighting, the core is heavily down-weighted, although the short spacings remain critical to restore the extended structure of the input model. In the input model, the source emission extends over $\sim 40''$. This is less than the LAS of the core ($0.85\lambda/b_{min} \sim 170''$) so we expect to be able to accurately recover all structures.

We perform a 6 hour synthesis simulation, and a 10 min snapshot observation for each configuration. We then examine the PSF properties, the image dynamic range, and the image fidelity. The dynamic range is defined as: (peak surface brightness/RMS noise). The fidelity is defined for each image pixel as in memo #64 [1] as: (Image - Model)/Model, where the model is convolved with the same fitted beam as the image for the calculation. Figure 24 shows the uv-coverage for the snapshot and 6 hour syntheses.

Figure 25 shows example images from the 7-arm spiral+rest of the Core simulation for the 6 hour synthesis. The resulting image represents a very good recovery of the input model, and the fidelity is generally high. This conclusion is true for all the tests employed, hence we only include one example of the images for reference.

The synthesized beams are shown in Figure 26 for the 6 hour synthesis, and in Figure 27 for the 10 min snapshot. The parameters for the beams are given in Table 1, including: Gaussian fit FWHM parameters, and beam minimum and maximum sidelobes. The 7-arm spiral+rest of the Core performs best, in terms of maximum sidelobe levels, by about 50% for the 6 hour synthesis, and a factor two for the snapshot. The performance of the Lily Pad+rest of the Core and the current Plains+Core are similar, as expected given the uniform weighting scheme.

Table 2 gives the image performance parameters, including total recovered flux density, RMS noise off-source (strictly due to imaging artifacts), peak negative surface brightness, peak surface brightness, dynamic range (Peak/RMS), and fidelity. The fidelity is calculated over a box the includes the full source, and just the tail of the radio lobe (ie. without the hot spots). The values listed for fidelity include the mean fidelity ratio (unity would be a perfect match between model and simulated observation), and the rms scatter in that ratio over

the region in question. Larger scatter means more deviations between model and data due to imaging artifacts. Table 2 also gives image fidelity values f_{proj} using the flux-weighted metric summed over image pixels which has been adopted by the ngVLA project [8, 4]; for more discussion on this metric see ngVLA memo #67 [3]. This metric is evaluated as a flux-weighted sum over a specified region of interest (or out to the 10% point of the primary beam); in this case we evaluate over the entire imaged region, $\sim 40''$ in width. Similar to the metric used in ngVLA memo #64 [1] this metric has a limiting “perfect” value of 1.0. Both metrics suggest that, at least for the idealized case considered, all of these configurations deliver images which accurately represent the surface brightness of the radio sky to within $\sim 0.5\%$ on average.

We evaluate the accuracy with which flux is recovered as a function of angular scale by using a peak finding heuristic to identify peaks (30 to ~ 100) in each simulated image, and calculating the median fraction of integrated flux recovered in a circular aperture compared to the simulation input image as a function of aperture radius. These curves are shown in Figure 28. Most configurations considered recover the input flux to better than 1% at all scales; snapshots with the 7 arm spirall+rest of the Core perform slightly worse, consistently missing $\sim 1\%$ of the total flux. This is presumably due to the smaller number of short baselines in this configuration, but in any case it is well within the bounds of acceptable performance.

Considering imaging performance, the 7-arm spiral+rest of the Core array performs best in most parameters, while the results between the current Plains+Core (i.e., 5-arm spiral+rest of the Core) and Lily Pad+rest of the Core configuration are similar. The 7-arm spiral+rest of the Core has the best peak negative surface brightness, by about a factor 2. In all cases, the image dynamic range is high, ranging from around 6000 for the original Plains+Core and Lily pad+rest of the Core snapshot observations, to close to 10^5 for the 7-arm+rest of the Core 6hr synthesis observation. Recall that no thermal noise has been added. In all cases, the RMS noise due to imaging artifacts is orders of magnitude above the expected thermal noise, thereby validating the use of uniform weighting in this case.

In terms of image fidelity, all of the images show excellent fidelity, with mean values within 1% of unity, and with RMS scatter relative to the input model of 0.2% to 0.3% for the synthesis, and 1% to 3% for the snapshot. The 7-arm spiral+rest of the Core performs a factor ~ 2 to 3 times better in image fidelity RMS relative to the other configurations, in the snapshot observations. The improvement for the 6 hour synthesis observations is less marked. The 7-arm spiral+rest of the Core does show a slightly lower mean ratio, 0.991 vs. 0.997, for the snapshot imaging. This likely relates to the larger number of long baselines. However, again in all cases, the mean fidelity is very close to unity.

Overall, for image dynamic range and fidelity for high dynamic range imaging of a complex source using uniform weighting, the 7-arm spiral+rest of the Core performance is superior by a factor of 1.5 to 2, when synthesis is included in the observation. We note that synthesis could be done as a function of time or frequency, although we have not considered the latter. This conclusion is not surprising, given that even for a 5-arm spiral+rest of the Core, the arms are only separated by 20% in angle around the circumference, and hence a 20%

Table 1: Rev C Configuration Components

Configuration	Beam Fit	Sidelobe	Sidelobe
	FWHM (Arcsec)	Max	Min
Plains+Core 6hr	$0.27 \times 0.27, 71.5^\circ$	0.0082	-0.0060
7arm+rest of the Core 6hr	$0.26 \times 0.26, -87.8^\circ$	0.0050	-0.0017
Lily Pad+rest of the Core 6hr	$0.27 \times 0.26, 69.7^\circ$	0.0075	-0.0065
Plains+Core 10min	$0.28 \times 0.25, 67.4^\circ$	0.060	-0.038
7arm+rest of the Core 10min	$0.28 \times 0.27, -85.0^\circ$	0.030	-0.039
Lily Pad+rest of the Core 6hr	$0.27 \times 0.25, 64.9^\circ$	0.063	-0.038

Table 2: Rev C Configuration Components

Configuration	total	RMS	Minimum	Peak	DNR	Fidelity: All	Fidelity: Lobe	f_{proj}
	Jy	mJy/beam	mJy/beam	Jy/beam	Peak/RMS	Mean, RMS	Mean, RMS	
Plains+Core 6hr	240.1	0.14	-0.66	10.1	70600	0.996 ± 0.0024	0.997 ± 0.0032	0.995
7arm+rest of the Core 6hr	240.0	0.10	-0.49	9.5	88800	0.997 ± 0.0022	0.997 ± 0.0027	0.996
Lily Pad+rest of the Core 6hr	240.5	0.26	-1.2	10.0	38500	0.996 ± 0.0033	0.997 ± 0.0044	0.996
Plains+Core 10min	240.4	1.9	-11.7	10.0	5260	0.997 ± 0.032	0.997 ± 0.037	0.994
7arm+rest of the Core 10min	238.9	1.2	-6.1	10.6	8800	0.991 ± 0.013	0.993 ± 0.017	0.995
Lily Pad+rest of the Core 10min	240.7	1.6	-10.1	9.6	6000	0.997 ± 0.032	0.998 ± 0.051	0.994

synthesis in frequency or time will fill in the gaps between arms. The 7-arm spiral+rest of the Core performance becomes clearer in snapshot, narrow band imaging, by a factor of 2.5 in image fidelity.

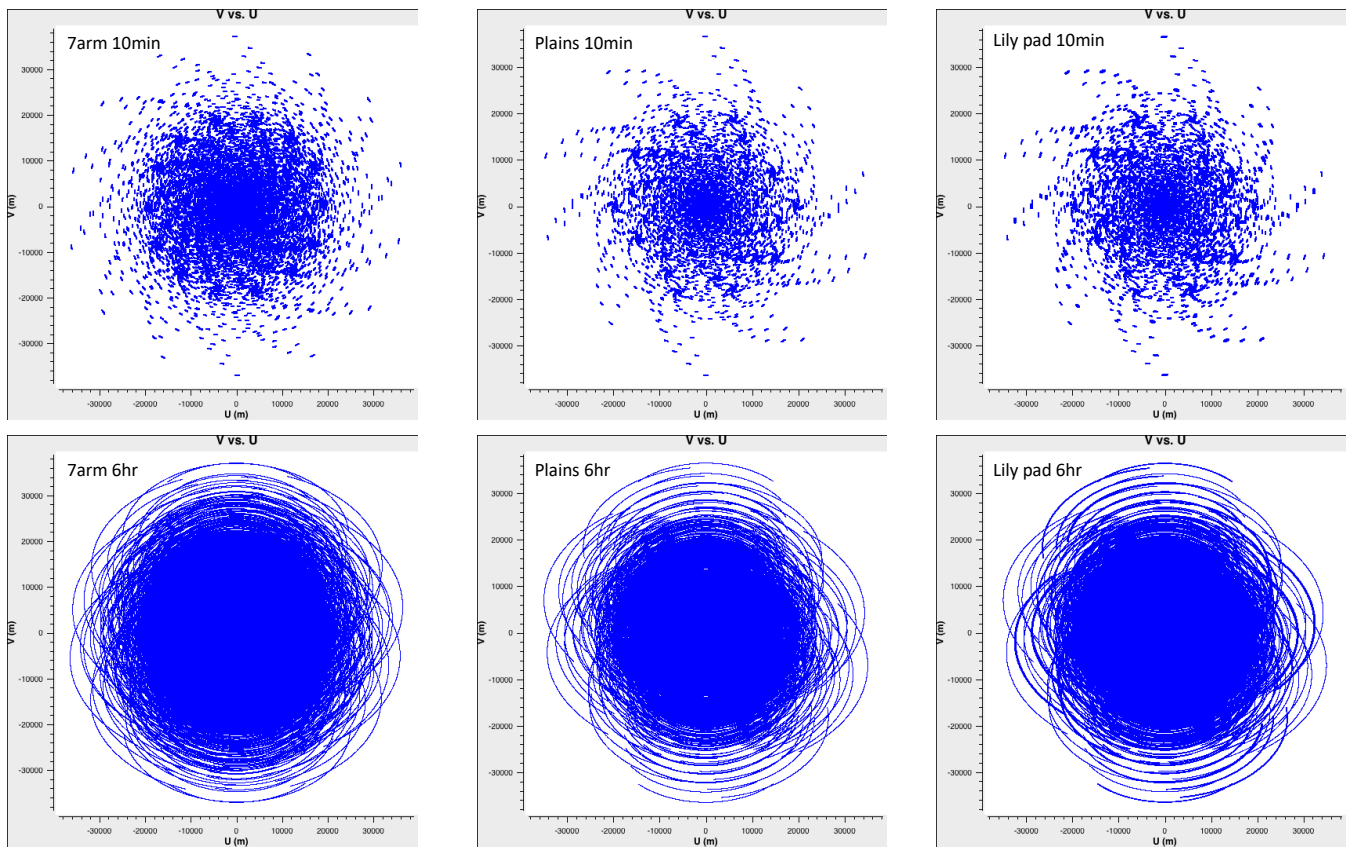


Figure 24: The uv-coverage of the 7arm (left) and Plains (right) configurations. Top is the 10min snapshot coverage, bottom is the 6hr synthesis.

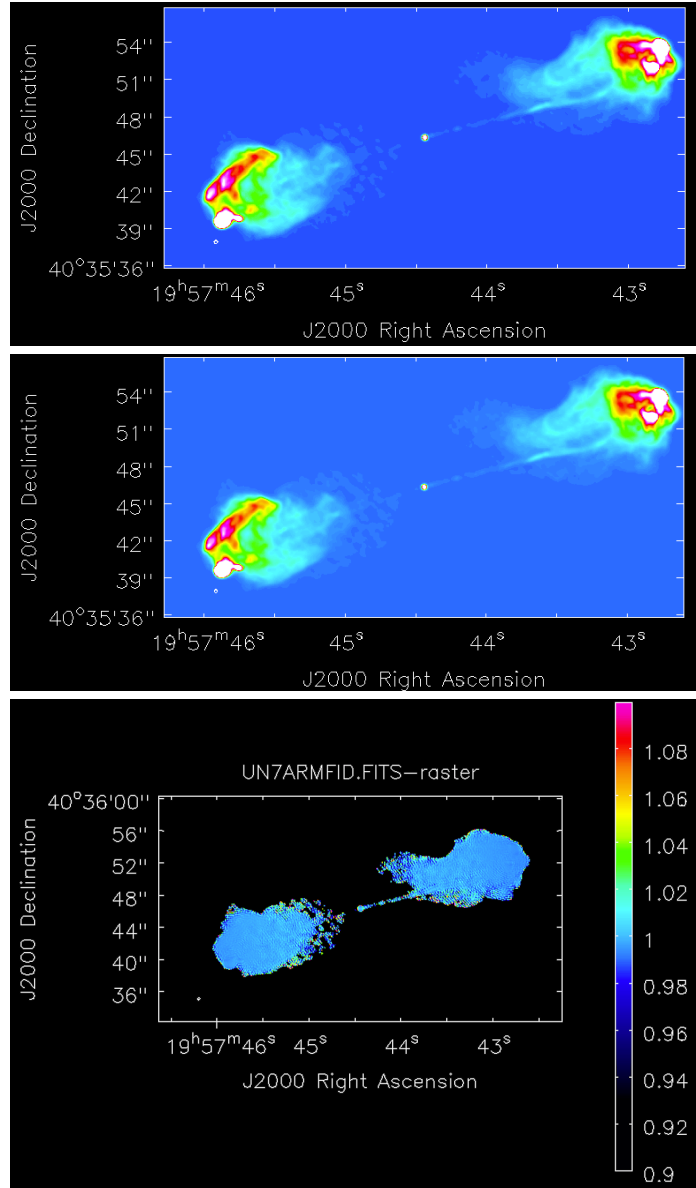


Figure 25: Images of the Cygnus A model and simulation. Top is the input sky model. Middle is the image made with the 7arm spiral plus core for a 6hr synthesis. Bottom is the fidelity = $(\text{image} - \text{model})/\text{model}$, blanked at 10σ . The fidelity color scale ranges from 0.9 to 1.1.

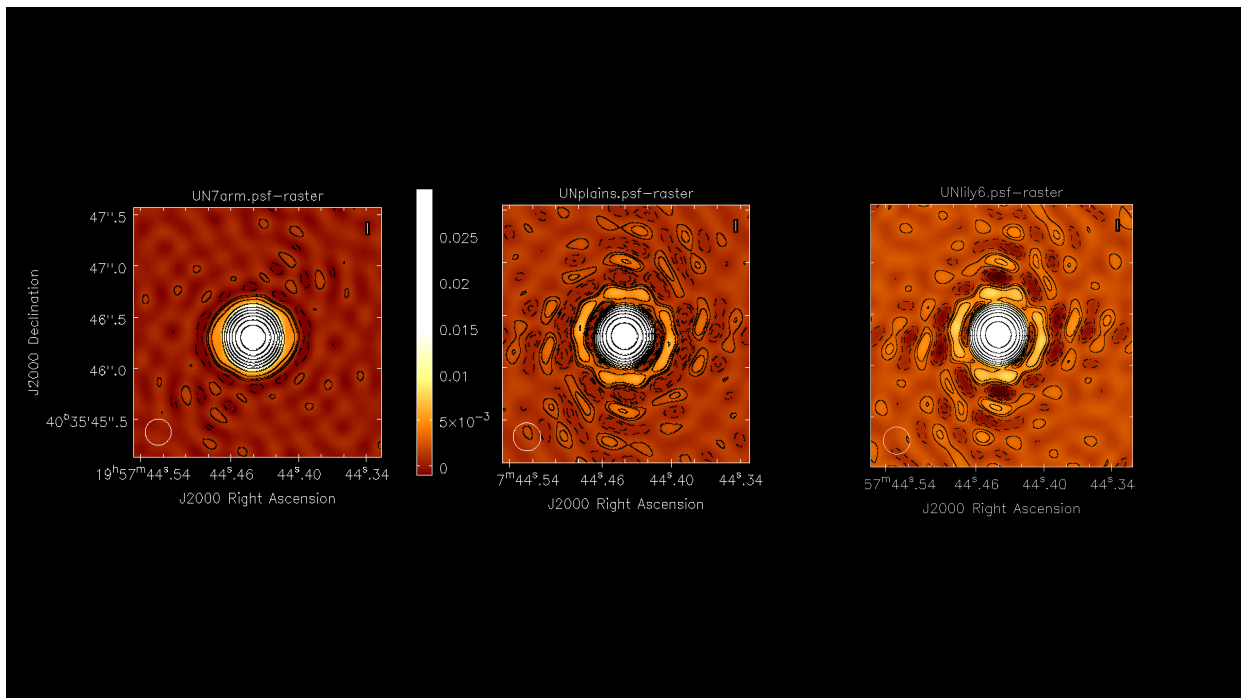


Figure 26: Images of the PSF for the Uniform weighted, uvtapered synthesized beam for the 6hr synthesis. Left is for the 7arm spiral; center is the 5arm spiral; right is Lily Pad. The contour levels are a logarithmic progression in factor of two, starting at 0.001. Negative contours are dashed.

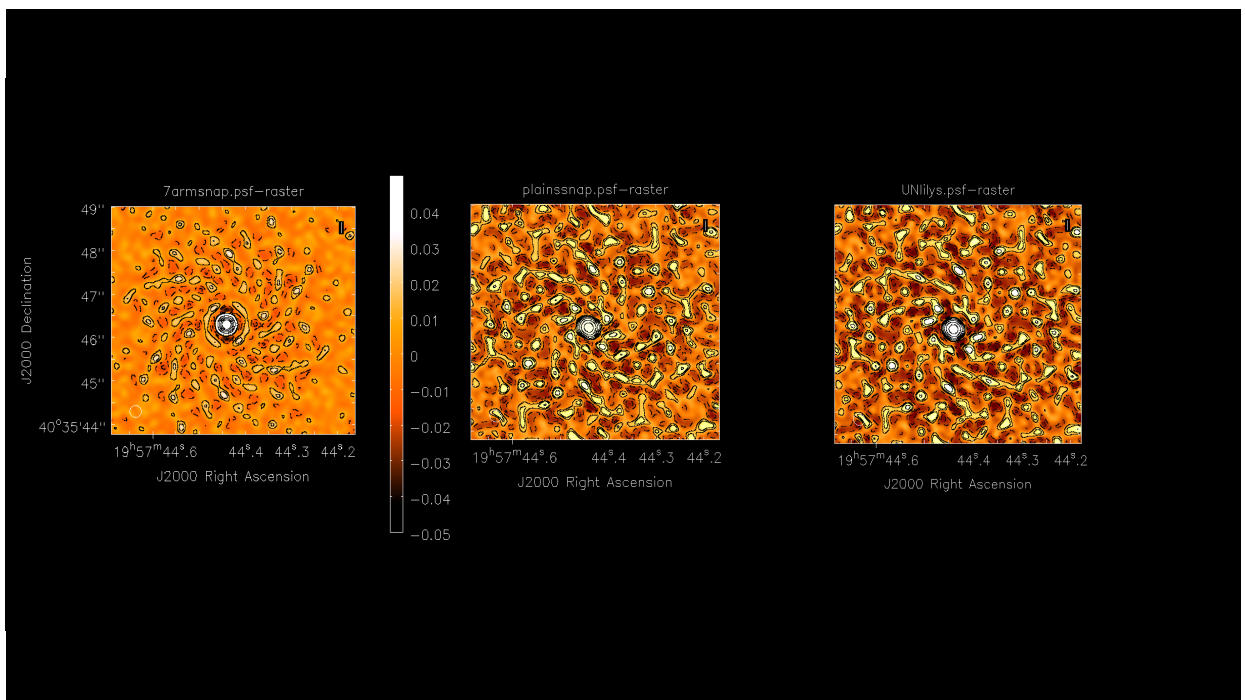


Figure 27: Images of the PSF for the Uniform weighted, uvtapered synthesized beam for the 10min synthesis. Left is for the 7arm spiral; center is the 5arm spiral; right is the Lily Pad. The contour levels are a logarithmic progression in factor of two, starting at 0.01. Negative contours are dashed.

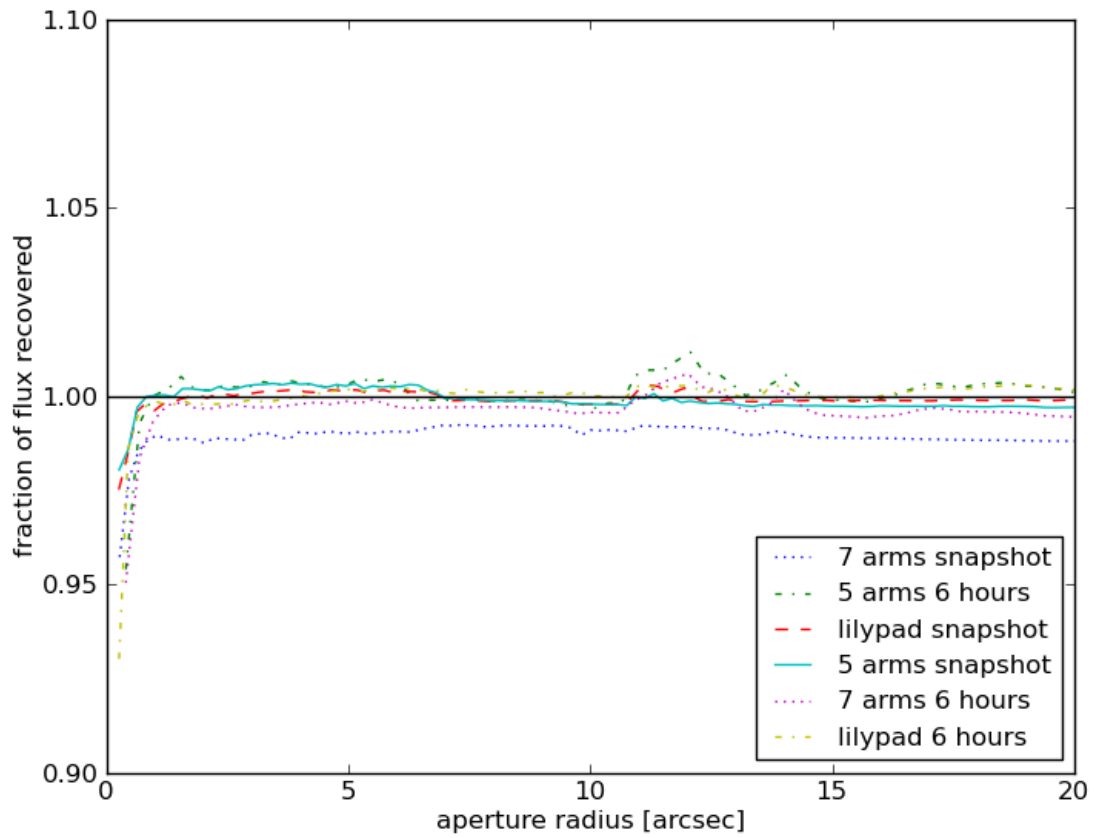


Figure 28: Median fraction of spatially integrated flux density recovered as a function of aperture diameter for all configurations considered.

4 Conclusions

- Both alternative subarrays redistribute a third of the collecting area from the Core to the Plains resulting in a factor 2 improvement in the level of the naturally weighted PSF skirt when used together with the remainder of the Core, compared to the current Plains+Core subarray. This means that the expected beam sculpting penalty should be less severe.
- The taperability curves for the 7-arm and the Lily Pad subarrays, when used with the rest of the Core, are more efficient at higher resolutions but less efficient at lower resolutions than the current Plains+Core. The resolution range over which these are more efficient is relatively small (less than a factor of 2 in resolution), while the range over which they are less efficient is significantly larger (about a factor of 10). When considered together with the beam sculpting penalty, it is likely that these effects will balance out.
- Comparing just the two alternative subarrays, regardless of being used together with the rest of the Core or stand alone, the Lily Pad subarray is slightly more efficient at higher resolutions and the 7-arm subarray is slightly more efficient at lower resolutions. The PSF of the Lily Pad has higher sidelobes but this could probably be improved by further optimization.
- Comparing just the two alternative subarrays, regardless of being used together with the rest of the Core or stand alone, the Lily Pad provides a larger number of short baselines ($< 200\text{m}$) compared with the 7-arm. This is specially true for the stand alone comparison for which the 7-arm provides no short baselines while the Lily Pad short baselines meet the LAS requirements of several of the science cases in ROP. This would allow the Lily Pad to be used for one observation while the rest of the Core could be used simultaneously for a different observation.
- For performance when imaging a complex, extended source with uniform weighting, the 7-arm spiral array performs best in all parameters (synthesized beam sidelobes, peak negative surface brightness, dynamic range), while the results between the 5-arm spiral and Lily Pad configuration are similar. The 7-arm spiral has the best peak negative surface brightness, by about a factor 2, and a higher dynamic range, by a factor 1.5 to 2, depending on synthesis.
- In terms of image fidelity, all arrays consider accurately reconstructed the input sky brightness to within $\sim 0.5\%$. The 7-arm spiral performs slightly better in terms of consistency, with a factor of 2.5 times lower variation in fidelity over the image compared to the other configurations for snapshot observations (1.5x lower for a 6 hour track).
- All array configurations recovered input structures as a function of angular scale accurate within $\sim 1\%$ up to $40''$, with the current plains and lily-pad arrays performing slightly better for snapshot observations

References

- [1] Chris Carilli, Joe Carilli, Alan Erickson, et al. *Next Generation Very Large Array Memo No. 64 High Dynamic Range Imaging*
- [2] Chris Carilli, *Next Generation Very Large Array Memo No. 82 Configuration: Reference Design RevC.01 Description and Alterations.*
- [3] Brian Mason, *Next Generation Very Large Array Memo No. 67: Demonstration & Analysis of ngVLA core + Short Baseline Array Extended Structure Imaging.*
- [4] Eric Murphy et al. *ngVLA Science Requirements (020.10.15.05.00-0001-REQ-B)*
- [5] Viviana Rosero, *Next Generation Very Large Array Memo No. 55 Taperability Study for the ngVLA and Performance Estimates.*
- [6] Viviana Rosero, *Next Generation Very Large Array Memo No. 72 A Study of ngVLA Subarray Efficiency: Plains + Fractions of the Core.*
- [7] Viviana Rosero, *Next Generation Very Large Array Memo No. 76 Subarray Selection for the Reference Observing Program.*
- [8] Rob Selina, et al., *ngVLA System Requirements (020.10.15.10.00-0003-REQ)*